Research Article

Caries Research

Caries Res
DOI: 10.1159/000501901

Received: December 6, 2018
Accepted after revision: July 3, 2019
Published online: September 11, 2019

T_2 Mapping as a Tool for Assessment of Dental Pulp Response to Caries Progression: An in vivo MRI Study

Ksenija Cankar[a] Jernej Vidmar[a, b, d] Lidija Nemeth[c] Igor Serša[a, d]

[a]Institute of Physiology, Faculty of Medicine, University of Ljubljana, Ljubljana, Slovenia; [b]Institute of Radiology, University Medical Center Ljubljana, Ljubljana, Slovenia; [c]Department of Dental Diseases and Normal Dental Morphology, Faculty of Medicine, University of Ljubljana, Ljubljana, Slovenia; [d]Jožef Stefan Institute, Ljubljana, Slovenia

Keywords
Dental pulp · Caries · MRI · T_2 mapping · ICDAS

Abstract
Among radiological methods, magnetic resonance imaging (MRI) excels in its ability to image soft tissue at great contrast and without the need of harmful radiation. This study tested whether in vivo MRI based on standard MRI sequences run on a standard clinical MRI system can be used to quantify dental pulp response to caries progression using the T_2 mapping method. In the study, 74 teeth were scanned on a 3-T MRI system, and caries was assessed according to the International Caries Detection and Assessment System (ICDAS). The T_2 maps were processed to obtain T_2 profiles along selected root canals (from crown to apex), and the profiles were sorted according to both tooth type (single-rooted vs. molar) and ICDAS score. In all the examined dental pulps, it was found that T_2 values decrease with an increase in the ICDAS score. In the coronal part of dental pulps, average T_2 values of 166, 153, and 115 ms were found in ICDAS groups 0, 1–3, and 4–6, respectively. In single-rooted teeth, T_2 values were found approximately constant as a function of dental pulp depth, while in multi-rooted teeth, they were found increasing in the coronal part and decreasing towards the root apex. The study confirmed that T_2 mapping of dental pulp can be used to reliably quantify its response to caries progression and that it has a potential to become a complementary diagnostic tool to standard radiographic methods in the assessment of dental pulp response to caries.

Introduction

Dental caries is a complex multifactorial chronic infectious disease. The dynamic process of demineralization and remineralization of dental hard tissues is guided by several risk or protective factors. One of the main caries risk factors is the presence of acidogenic bacteria in the biofilm of dental plaque [Pitts, 2011; Pretty and Ekstrand, 2016]. Microorganisms subsequently trigger inflammatory responses in the dental pulp, which range from hyperaemia to reversible and irreversible inflammation of the pulp tissue [Martin, 2003]. Therefore, an early and accurate assessment of dental pulp tissue response to caries progression before the treatment decision is of utmost importance [Zero et al., 2011]. The degree of dental pulp inflammation and the remaining dentin thickness play a decisive role in the outcome of conservative pulp-saving

Ksenija Cankar
Institute of Physiology
Faculty of Medicine, University of Ljubljana
Zaloška 4, SI–1000 Ljubljana (Slovenia)
E-Mail ksenija.cankar@mf.uni-lj.si

treatment [Mjör, 2002; Murray et al., 2002]. In addition, promoting the resolution of dental pulp inflammation may provide a valuable therapeutic opportunity to ensure the sustainability of dental treatments [Farges et al., 2015].

Currently, standard clinical diagnostics of dental pulp response to caries progression relies on indirect evaluation based on clinical symptoms that are subjective and highly influenced by patients' threshold for pain. The visualization of dental pulp morphology and function is very important for treatment decisions [Pretty and Ekstrand, 2016]. However, with the standard diagnostic imaging methods, this is difficult to achieve, considering the small size of dental pulp and the complexity of the root canal system. Film-based or digital conventional radiographic techniques and cone beam computed tomography (CBCT) provide information on hard dental tissues only. Consequently, they can provide only the information on the enamel and dentin demineralization depth and its distance to the pulp chamber. Therefore, a non-invasive and accurate clinical diagnostic method to enable more precise assessment of dental pulp response to caries progression is of utmost importance. A possible candidate among radiological methods that is potentially capable of the task is magnetic resonance imaging (MRI).

MRI enables non-ionising, radiation-free imaging of all soft tissues in which hydrogen-containing molecules in a liquid environment are abundant. In addition, of all the standard diagnostic imaging techniques, MRI provides the best contrast among various soft tissues, being enabled by the different nuclear magnetic resonance (NMR) relaxation times T_1 and T_2 of the tissues. NMR relaxation times tell how fast protons excited by NMR radiofrequency pulses return to the equilibrium state. Average orientation of protons is represented by the physical quantity known as the proton nuclear magnetization. The longitudinal relaxation time T_1 is a characteristic time for the return of the magnetization along the static magnetic field of the NMR magnet, while transversal relaxation time T_2 is a characteristic time for the decay of the magnetization oriented perpendicular to the static magnetic field [Vlaardingerbroek and Boer, 1996]. MRI enables clear visualization of dental pulp morphology, as has been demonstrated by several studies on extracted human teeth [Sustercic and Sersa, 2012; Drăgan et al., 2016]. With newly developed imaging sequences that enable MR signal acquisition practically immediately after the signal excitation, hard dental tissues such as dentine can be MR imaged too [Idiyatullin et al., 2011; Weiger et al., 2012]. With respect to extracted human teeth, it has been shown that demineralization depth can be determined from T_1-weighted images and that this depth correlates with clinical caries as assessed and scored by the International Caries Detection and Assessment System (ICDAS) [Pitts, 2004] as also with the apparent diffusion coefficient (ADC), which is susceptible to tissue abnormalities [Vidmar et al., 2012]. In another study, the relevance of ADC mapping in discrimination and localization of intact and affected dental pulp regions in carious teeth was demonstrated [Cankar et al., 2014]. Similarly, it has been shown that the mapping of the transversal relaxation time (T_2 mapping) enables, without the need for a contrast medium, good differentiation among different stages of soft tissue inflammation [Bohnen et al., 2017] and is therefore an appropriate method for early detection of caries-induced dental pulp inflammation.

MRI of teeth can also be done in vivo [Idiyatullin et al., 2011; Hövener et al., 2012]. In an experimental animal model study of teeth, high-resolution anatomical MR images with diagnostic value comparable to those of CBCT were obtained [Gaudino et al., 2011]. In vivo MRI has also been used in the detection of dental pulp tissue necrosis after traumatic dental injuries [Assaf et al., 2015] and in the quantification of carious lesions by the use of a gadolinium-based, oral contrast medium [Tymofiyeva et al., 2009]. A resolution comparable to that of MR microscopy was obtained in an in vivo dental MRI study on humans by using a specially designed intraoral wireless dental coil [Ludwig et al., 2016].

In the present in vivo study, teeth of patients with caries of various ICDAS scores were MRI scanned by T_1-weighted and T_2 mapping MRI techniques. The obtained T_2 maps of different tooth types (single-rooted vs. multi-rooted teeth with different ICDAS scores) were analysed further for T_2 profiles along dental pulp with the aim of finding statistically significant differences among the T_2 values of different ICDAS scores at given dental pulp depths, thereby confirming that T_2 mapping can be used to detect structural changes in a dental pulp in vivo.

Materials and Methods

Patients

In the study, 12 volunteers (6 males and 6 females) that came to students' clinical practice for dental treatment were enrolled (mean age 34.4 ± 7.3). Patients ($N_c = 7$) with various stages of caries progression were prospectively enrolled. Caries-free age-matched volunteers ($N_h = 5$) were recruited as controls. In each of the enrolled patients, the clinical dental examination and the detection of caries lesions presence were interpreted by 2 independent calibrated clinical examiners using the ICDAS system. Both examiners had extensive clinical experience in restorative dentist-

ry and did not have access to any other information, such as patient identity or clinical history. All teeth of which dental pulps were clearly visible on T_2 maps were included in the study (approximately 6 teeth for each subject). In all, 74 teeth were examined (34 single-rooted and 40 multi-rooted) and assessed using conventional clinical probing and radiography and were classified according to the ICDAS system (Table 1): score 0, sound dental surface; score 1, first visual change in enamel; score 2, distinct visual changes in enamel; score 3, localised enamel breakdown; score 4, underlying discoloured dentin with or without localised enamel breakdown; score 5, distinct cavity with visible dentin; score 6, extensive distinct cavity with visible dentin. All carious lesions were on occlusal or proximal surfaces or on both surfaces combined. In addition, all carious lesions were classified as active, according to ICDAS visual and tactile activity criteria [Ekstrand et al., 2018]. Standard clinical dental pulp vitality tests (cold test with tetrafluoroethane and electric dental pulp test) were positive in all the examined teeth, and none of the teeth included in the study was symptomatic. Contraindications to dental MRI, such as an implanted pacemaker, constituted exclusion criteria. Each of the volunteers provided written informed consent to participate in this protocol, which was approved by the Ethical Committee of the National Ministry of Health and conformed to the STROBE guidelines.

MR Image Acquisition

MR imaging was performed on a 3-T whole-body MRI system (TX Achieva, Philips, Netherlands) with a maximal gradient strength of 80 mT/m and with the use of a 32-channel receiving head coil in all patients within 7 days after the initial examination. All patients were able to perform routine daily activities prior to each examination. The MR protocol consisted of a set of moderate-resolution images to localise the dental pulp anatomy first. Specifically, T_2-weighted turbo spin-echo imaging in the axial plane and fat suppressed proton density imaging in the coronal and sagittal planes were used to localise and visualise most of the pulp chamber. In the sagittal orientation, T_1-weighted images of the pulp were obtained using the spin-echo imaging sequence with parameters: repetition time (TR)/echo time (TE), 400/10 ms; single echo; field of view 140 × 140 mm^2; slice thickness 2 mm; image acquisition/reconstruction matrix 156 × 124/320 × 320; acquisition/reconstruction voxel size 0.9 × 1.12 × 2/0.44 × 0.44 × 2 mm^3; 5 slices; bandwidth 253 Hz/pixel; no signal acquisition acceleration and acquisition time of 3 min 25 s. For T_2 mapping, multi-spin-echo (MSE) T_2-weighted sequence in a single sagittal slice and with a field of view that covered most of the pulp chamber was employed. The parameters of the MSE sequence were: TR/TE, 2,000/15 ms as well as 30, 45, 60, 75, 90 ms; field of view 160 × 160 mm^2; slice thickness 2.5 mm; image acquisition/reconstruction matrix 380 × 311/560 × 560; acquisition/reconstruction voxel size 0.42 × 0.51 × 2.5/0.29 × 0.29 × 2.5 mm^3; single slice; bandwidth 290 Hz/pixel; no signal acquisition acceleration; and acquisition time for all 6 echoes was equal to 10 min 24 s.

MR Data Analysis

MSE images were used to calculate the corresponding maps of T_2 relaxation time by using the pixel-wise, mono-exponential, non-negative least-squares fit analysis that is implemented in the MRI Analysis Calculator plugin (ImageJ, National Institutes of Health, USA). Briefly, the routine takes as an input images of all echoes, and then for each pixel (i,j) in the images, analyses the measured signal decay $\tilde{S}_{i,j}(TE)$ with an increasing echo time TE using a model function assuming mono-exponential signal decay $S_{i,j}(TE) = S_{0\_i,j} \exp(-TE/T_{2\_i,j})$. The model function has 2 model parameters: $S_{0\_i,j}$ that corresponds to a pixel signal at $TE = 0$ and $T_{2\_i,j}$ which is a single pixel transversal relaxation time. Finally, from the best fit between the model function $S_{i,j}(TE)$ and experimental data $\tilde{S}_{i,j}(TE)$, values of the relaxation time T_2 in each pixel are calculated. Finally, from these a T_2 map is formed.

Calculated T_2 maps of dental pulps were processed by the ImageJ digital image processing software to obtain T_2 value profiles along dental pulps. The procedure is illustrated in Figure 1. First, a central line that followed the contour of the pulp or of the selected root canal was drawn manually. Then, 2-pixel (570 µm) high and dental-pulp-wide boxes were selected starting from the coro-

Table 1. Number of studied teeth by the ICDAS score and their type

Patient index	Sex	Age	ICDAS score – single-rooted teeth						
			0	1	2	3	4	5	6
1	Female	38	3						
2	Male	25	2	1					
3	Female	26	1						
4	Female	40	1		2				
5	Male	38	2						
6	Female	23	1		1	1	1	1	
7	Male	24		1		1	1		
8	Female	38							1
9	Male	39		2					2
10	Male	40				1	1	1	1
11	Female	29			1			1	
12	Male	32				1			2
Combined			10	4	4	4	3	3	6
Patient index	Sex	Age	ICDAS score – multi-rooted teeth						
			0	1	2	3	4	5	6
1	Female	38	5						
2	Male	25	1						
3	Female	26	3						
4	Female	40	2						
5	Male	38	2						
6	Female	23			1	2		2	
7	Male	24		2	1	1	1	1	
8	Female	38		1	2	2			1
9	Male	39				2	1		
10	Male	40			1				
11	Female	29						1	1
12	Male	32		1	1		1		1
Combined			13	4	6	7	3	4	3
Total			23	8	10	11	6	7	9

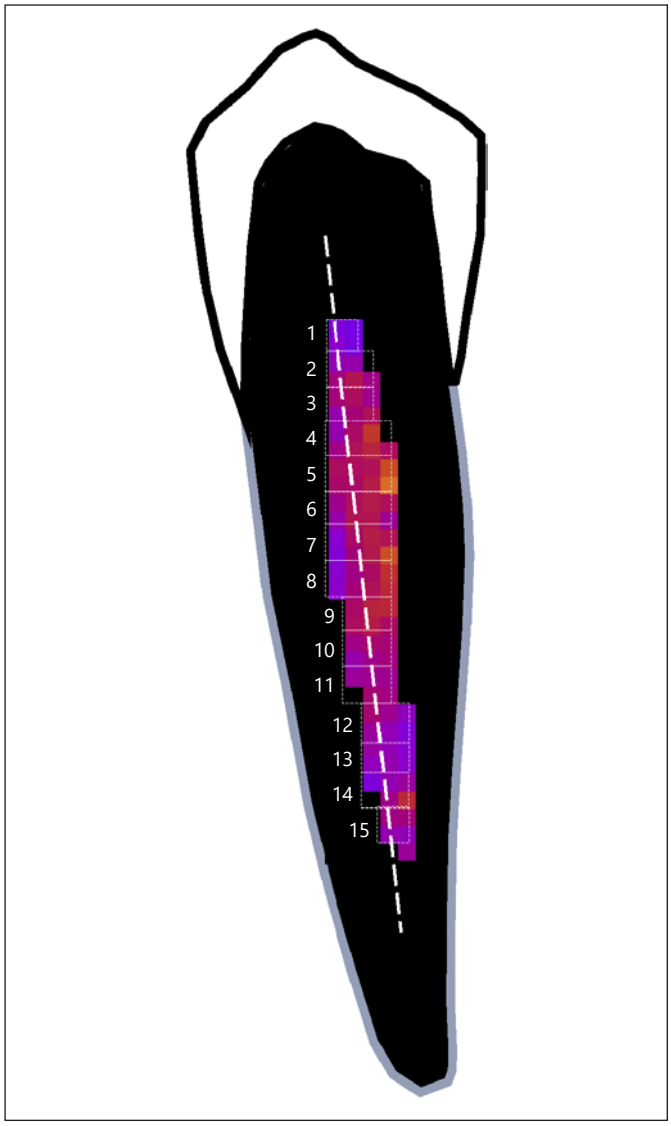

Color version available online

Fig. 1. An illustration of a dental pulp T_2 value profile measurement procedure. T_2 values were averaged in 2-pixel high and dental-pulp-wide boxes (excluding pixels with zero T_2 values) to obtain a noise-reduced T_2 value profile along the dental pulp from the coronal to the apical part.

nal part of the pulp and ending in the apical part of it. In the next step, T_2 values were averaged within each box to reduce the noise. In this step, pixels with zero T_2 values, which lay out of the pulp, were excluded from averaging. Thus obtained box-averaged T_2 values were used as T_2 value depth profiles in further analyses of the study. For a negative control, the dental pulp tissue of the necrotic teeth that had no detectable MRI signal was used.

Statistical Analysis

First, the teeth were divided between single- and multi-rooted teeth due to a different distribution of pulp tissue volumes. Namely, in single-rooted teeth, the pulp chamber volume is relatively small compared to multi-rooted teeth. In contrast, in multi-rooted teeth, the pulp tissue volumes in each root canal are relatively small compared to single rooted teeth. In each of the groups, teeth were additionally divided according to their ICDAS score: ICDAS score 0, ICDAS scores from 1 to 3, and ICDAS scores 4–6. The sample size was determined to be at least 3 teeth in each subgroup (Table 1) at power 0.8 and alpha value 0.05 (SigmaPlot 14.0, Systat Software, USA). The obtained T_2 relaxation times were compared among the groups of teeth with different ICDAS scores by way of analysis of variance (ANOVA) with the Bonferroni correction (Bonferroni's post hoc test). The results were expressed as mean values and SD of means, with the criterion of significance at $p < 0.01$.

In addition, the average T_2 relaxation time for each tooth was calculated along the dental pulp chamber in the coronal quarter, 2nd quarter, 3rd quarter, and apical quarter. The obtained T_2 relaxation times were compared among the groups of teeth with different ICDAS scores by way of Kruskal-Wallis ANOVA on ranks (H at least 25.474 with 6 degrees of freedom and $p < 0.001$) with the Dunn's post hoc test. The results were expressed as median values, 25 and 75% percentiles, with the criterion of significance at $p < 0.05$.

Results

An example of MR images of the upper and lower jaw of a 32-year-old male patient is presented in Figure 2 by a T_1-weighted image (a) and the corresponding T_2 map (b) in a sagittal plane. In the T_1-weighted image, all major structures in the oral cavity can be seen; while hard dental tissues do not produce any detectable MR signal in the image unless they are demineralised, soft dental tissues, that is, dental pulps and periodontal tissues, produce a detectable MR signal. The image can help in the assessment of dental pulp anatomy; however, it is not very sensitive to tissue changes associated with inflammation processes such as pulpitis. For the latter purpose, the T_2 map is much better. In the map, 2 regions with carious teeth are identified and are indicated by dashed rectangles. In Figure 2e, a magnified image of region c with the dental pulp of a single-rooted tooth with caries is shown; while in Figure 2f, a magnified image of region d with the dental pulp of a molar with caries is presented. Figure 2e and f show the corresponding 1D profiles of T_2 values along the dashed line in the image of the pulp. Both teeth have low T_2 values of <100 ms in the pulp region, which is characteristic for changes in dental pulp tissue morphology. The values are more constant with the single-rooted teeth than with the multi-rooted teeth and can at some points reach 150 ms or more. With dental pulp of both tooth types, T_2 values tend to decrease towards the root apex. The decrease in T_2 values as well as high T_2 values in

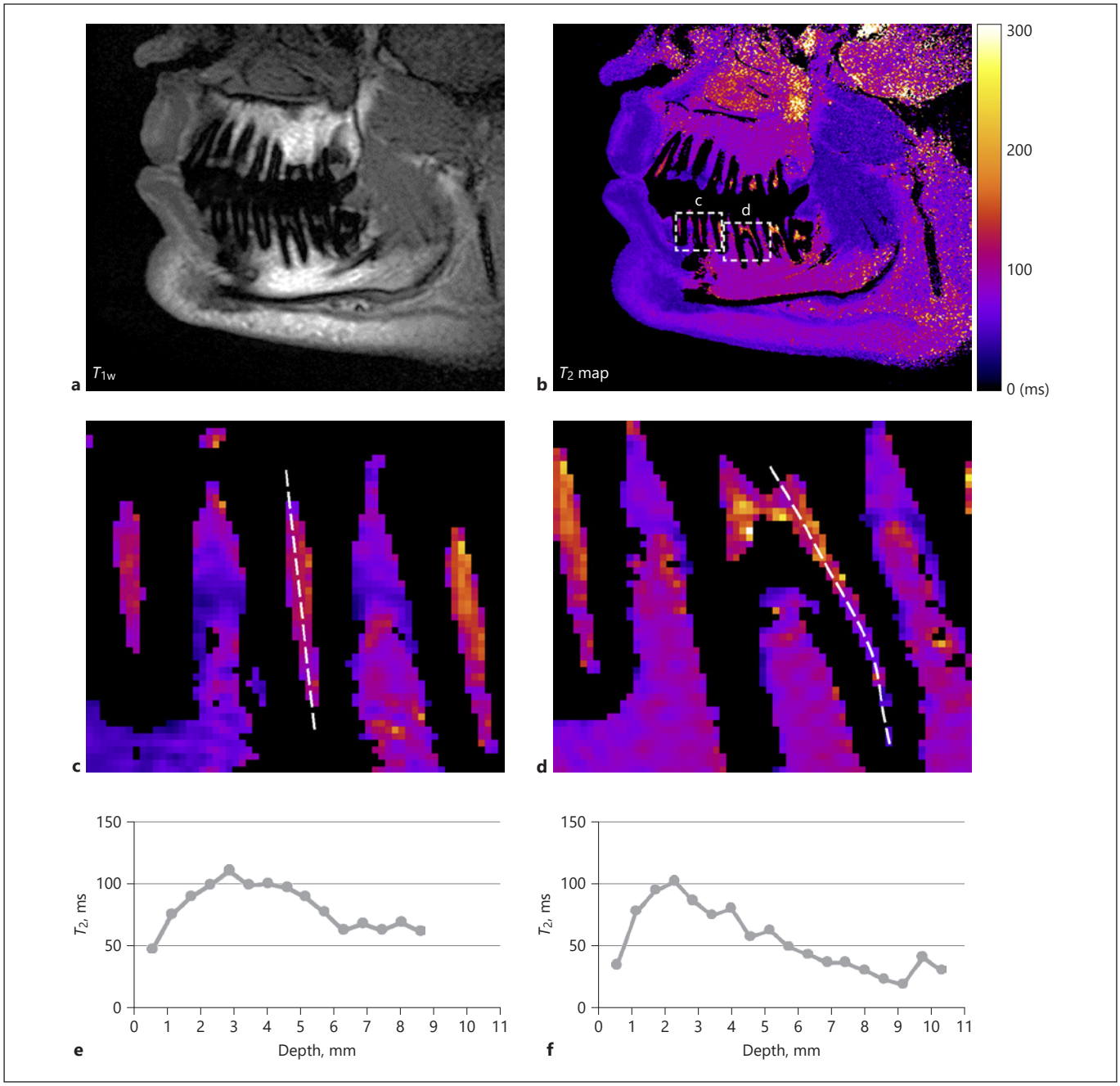

Fig. 2. T_1-weighted image (**a**) and the corresponding T_2 map (**b**) of a representative patient's teeth in a sagittal slice. In the T_2 map, 2 regions of interest (ROI) are indicated by a dashed line, one is containing a single-rooted tooth and the other a molar. The magnified ROIs are shown in panels **c** and **d**, respectively. **e**, **f** Graphs of dental pulp T_2 value depth profiles that were measured along a dashed line central to the dental pulp as indicated in the corresponding T_2 maps of the ROIs.

multi-rooted teeth can be a consequence of the partial volume effect, that is, an effect to the voxel signal in cases where the investigated tissue only partially fills the voxel [Vlaardingerbroek and Boer, 1996]. In a multi-rooted tooth, healthy and affected dental pulp tissue can be present within a single voxel, but at the dental pulp apex, the width is less than the size of a pixel.

T_2 map calculation procedure, using an example from Figure 2d, is illustrated in Figure 3. First, from a series of differently T_2-weighted images (Fig. 3a), mea-

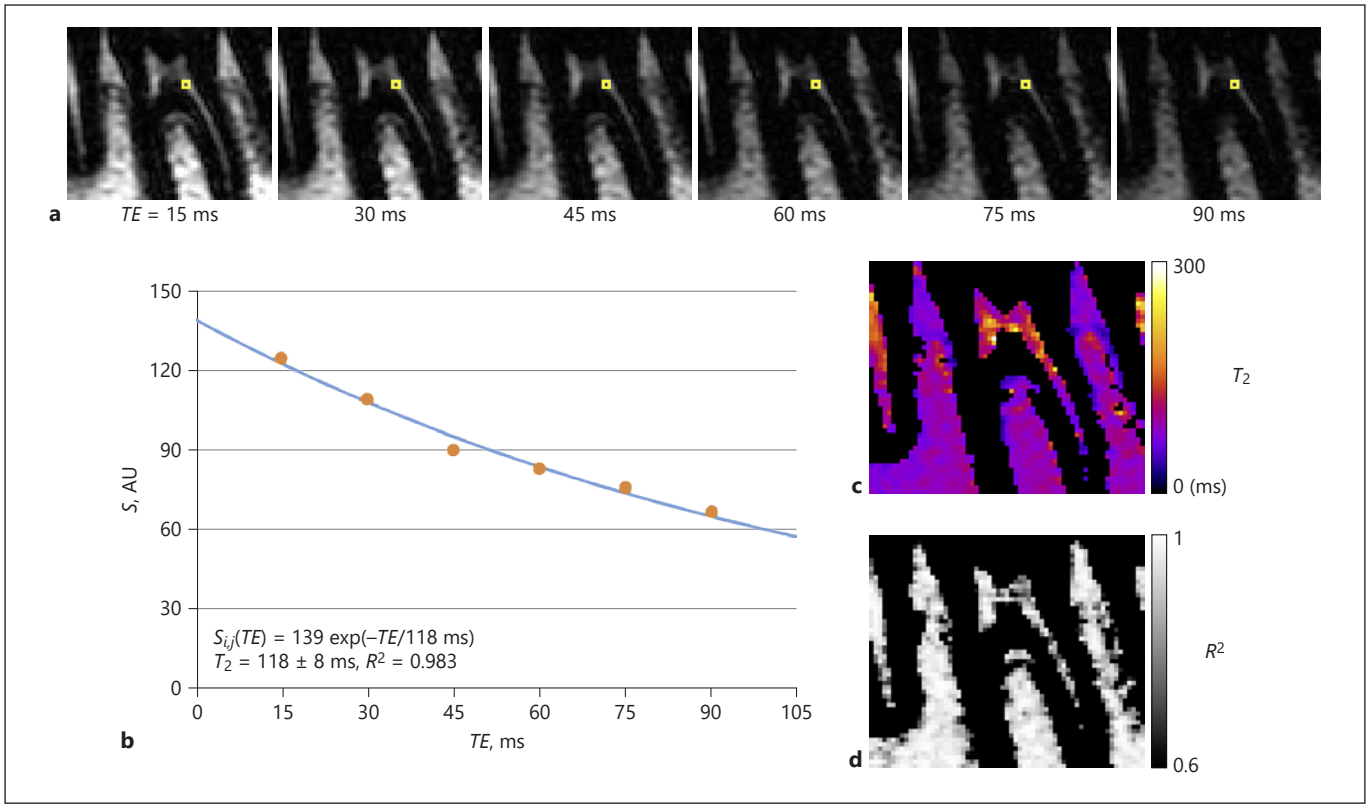

Fig. 3. An example of T_2 map calculation procedure. **a** From a series of differently T_2-weighted images, a signal from an individual pixel (*i,j*; encircled in yellow) as a function of echo time is extracted. **b** The measured signals (orange dots) are then analysed by the mono-exponentially decaying model function $S_{i,j}(t) = S_{0\_i,j} \exp(-t/T_{2\_i,j})$, and from the best fit between the experimental data and the model function, that is shown by the blue curve in the graph, the best fit model parameters $S_{0\_i,j}$ and $T_{2\_i,j}$ are extracted. By repeating this procedure for each pixel of the T_2-weighted image series, a T_2 map (**c**) and the corresponding map of the coefficient of determination (**d**) are calculated.

sured signal intensity $\tilde{S}_{i,j}(TE)$ from the selected image pixel as a function of echo time *TE* is extracted. This is shown in the graph in Figure 3b by orange dots. In the same graph, the model function $S_{i,j}(t)$ having the best fit to the measured signals is shown by a continuous blue curve. The best fit model parameters of the model function are equal to $S_{0\_i,j} = 139 \pm 4$ and $T_{2\_i,j} = 118 \pm 8$ ms, while the corresponding coefficient of determination is equal to $R^2 = 0.983$. The results of T_2 calculation for some additional image pixels are shown in online supplementary Figure S1 (for all online suppl. material, see www.karger.com/doi/10.1159/000501901). By repeating this procedure for each pixel of the T_2-weighted image series, a T_2 map was calculated (Fig. 3c) as well as the corresponding map of the coefficient of determination (Fig. 3d).

In Figure 4, dependence of T_2 relaxation time on the depth along the dental pulp is shown separately for single-rooted teeth (a) and for multi-rooted teeth (b). For both tooth types, the dependence is plotted for 3 ICDAS groups: intact teeth (ICDAS score 0), teeth with early caries lesion in enamel (ICDAS scores 1–3), and teeth with severe caries destruction in enamel and dentin (ICDAS scores 4–6). From the graphs, it can be seen that with both tooth types, the intact group (ICDAS 0) has the highest T_2 values, which can for some teeth reach 170 ms or more. In the case of caries, the T_2 values of single-rooted teeth decreased by 10–30 ms in the ICDAS 1–3 group, and they decreased further by 10–30 ms in the ICDAS 4–6 group, that is, a decrease of 20–60 ms (ANOVA, Bonferroni's post hoc test, $p < 0.001$). With multi-rooted teeth, no decrease was observed in the ICDAS 1–3 group, and a larger decrease of 20–40 ms was observed in the ICDAS 4–6 group. T_2 values of <120 ms are a clear indication of a dental pulp response to caries.

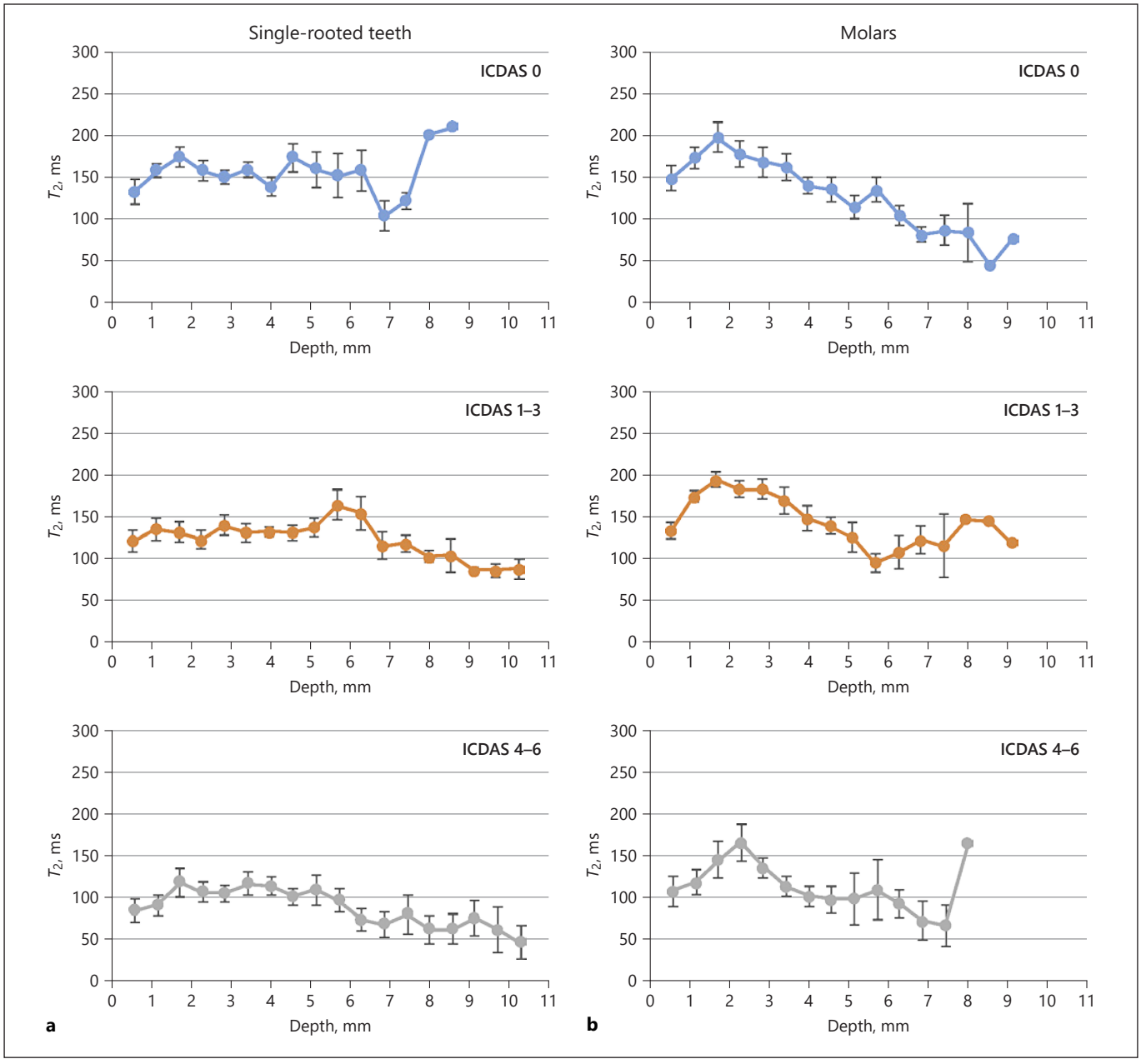

Fig. 4. Distribution of average T_2 relaxation times (obtained from corresponding T_2 maps) along the dental pulp of intact teeth (ICDAS score 0), of teeth with an early caries lesion (ICDAS scores 1–3), and of teeth with a severe caries lesion (ICDAS scores 4–6) in single-rooted teeth (**a**) and in multi-rooted teeth (**b**).

Graphs in Figure 5 depict measured T_2 value (data from Fig. 4) as a function of the ICDAS score for 4 different dental pulp regions: coronal quarter (a, depth 0–2.3 mm), 2nd quarter (b, depth 2.3–4.6 mm), 3rd quarter (c, depth 4.6–6.9 mm), and apical quarter (d, depth 6.9–10.3 mm). For the graphs, data of both tooth types, single- and multi-rooted, were included. In all the graphs, a trend of decreasing T_2 values with increasing ICDAS scores can clearly be seen. The trend is different in the first half of the pulp (coronal and 2nd quarter) than in the second (3rd and apical quarter). For the first 2 quarters, T_2 values are almost constant up to ICDAS 4 and then rapidly decrease with ICDAS 5 and 6; while for the last 2 quarters, T_2 values decrease more uniformly

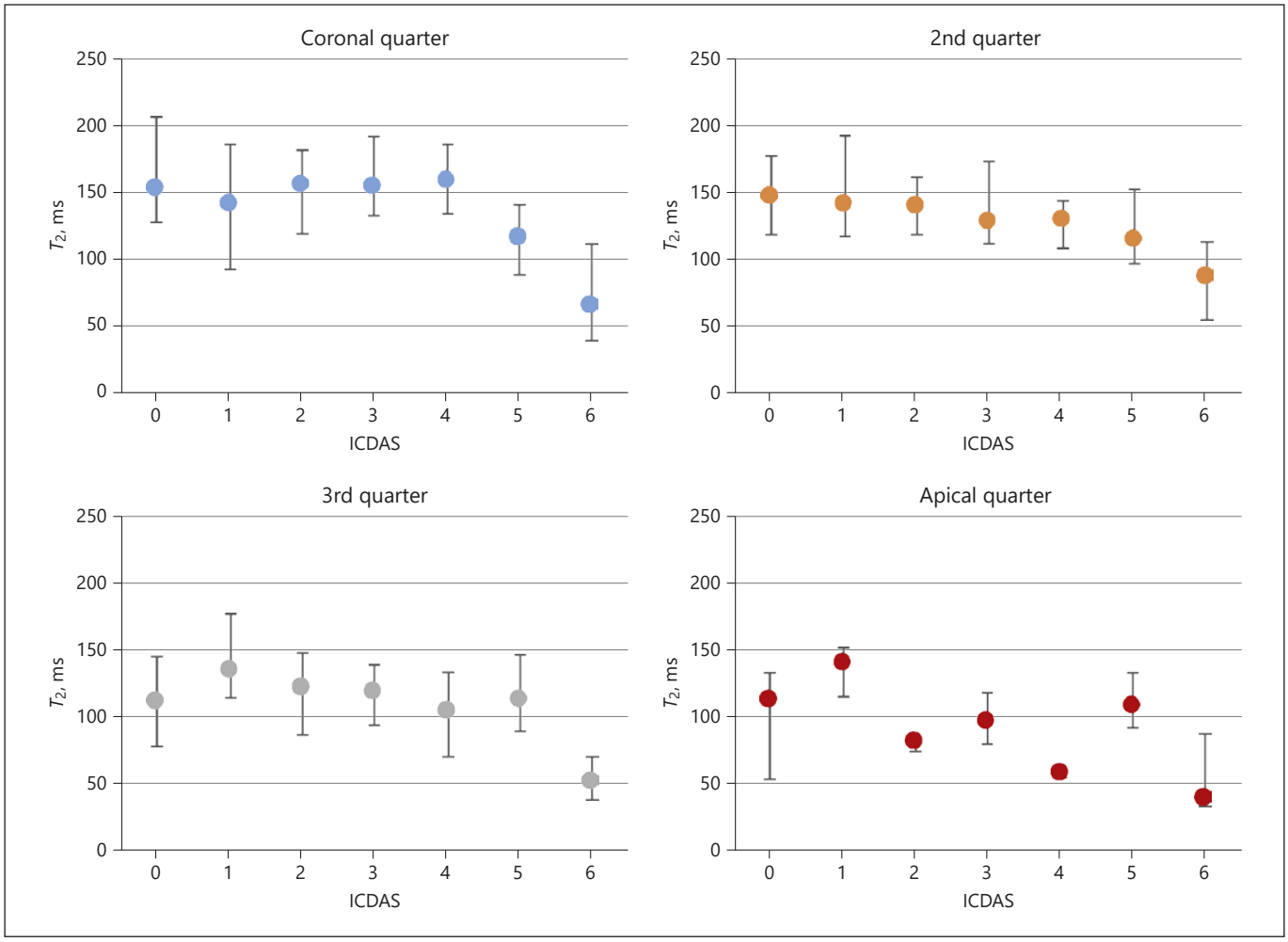

Fig. 5. Average T_2 relaxation times (obtained from corresponding T_2 maps) in the dental pulp of carious teeth as a function of the ICDAS score and position along the dental pulp tissue towards the apex: coronal quarter, 2nd quarter, 3rd quarter, and apical quarter. All teeth, single- and multi-rooted, were included in the analysis.

with ICDAS scores. In all 4 quarters of dental pulp, the differences in mean T_2 values among the groups of teeth with different ICDAS scores are statistically significant (ANOVA, $p < 0.05$). Statistical analysis of the data in Table 2 shows that the ICDAS 6 group is significantly different from all other ICDAS groups except ICDAS 5 in the coronal region, 2nd quarter, and 3rd quarter. In the 3rd quarter, the ICDAS 6 group is also significantly different from the ICDAS 5 group. In the apical quarter, only a significant difference between the ICDAS 6 group and the ICDAS 1 group was observed. A notable difference was also found between the ICDAS 5 and ICDAS 0, ICDAS 3, and ICDAS 4 groups in the coronal region, while differences between other group pairs were non-significant.

Discussion

The aim of the present in vivo study was to assess the feasibility of T_2 mapping for detection of structural tissue changes in dental pulp in response to caries progression. The study was performed in patients with teeth with various stages of caries on a standard 3-T MRI system by using standard of care MR imaging methods. The results of the study confirmed that it is possible to distinguish between intact and affected dental pulp regions based on T_2 values and that those values correlate well with the severity of caries according to its ICDAS score. It was found that for any dental pulp depth and for any tooth type, intact teeth (ICDAS 0) have approximately 40 ms higher T_2 values than severely caries-affected teeth (ICDAS 4–6;

Table 2. All pairwise statistical comparisons among T_2 values in the dental pulp of carious teeth with different ICDAS scores and in different positions along the dental pulp

ICDAS	ICDAS					
	0	1	2	3	4	5
Coronal quarter						
6	<0.001	<0.001	<0.001	<0.001	<0.001	1
5	<0.001	0.865	0.079	0.011	0.027	
4	1	1	1	1		
3	1	1	1			
2	1	1				
1	1					
2nd quarter						
6	<0.001	<0.001	<0.001	<0.001	0.036	0.096
5	0.200	0.605	1	1	1	
4	1	1	1	1		
3	1	1	1			
2	1	1				
1	1					
3rd quarter						
6	<0.001	<0.001	<0.001	<0.001	0.044	<0.001
5	1	1	1	1	1	
4	1	1	1	1		
3	1	1	1			
2	1	1				
1	1					
Apical quarter						
6	0.103	<0.001	1	0.180	1	0.074
5	1	1	1	1	1	
4	1	0.429	1	1		
3	1	1	1			
2	1	0.498				
1	1					

data from graphs in Fig. 4). Since MRI is an imaging modality, it enabled measurement of T_2 profiles along the dental pulp, also then providing a spatially resolved assessment of the pulp response to caries. Until now, it was not possible to obtain such findings, given the use of other radiological methods in earlier studies.

The range of T_2 values of a dental pulp can span over 50 ms, that is, from <100 ms in the case of teeth most severely affected by caries and up to 160 ms or more in the case of intact teeth (ICDAS 0). These findings are in agreement with observations from our previous ex vivo study which showed good agreement between MRI results and findings from a histological analysis of identical teeth [Cankar et al., 2014]. In teeth with extensive distinct cavities with exposed dentin, ADC values of the dental pulp were significantly lower than those of intact teeth. Histological analysis of the teeth revealed the presence of affected odontoblastic layers and thus confirmed significant progression of dental pulp inflammation. The results of our previous ex vivo study also showed that ICDAS score 6 with decreased MRI signal correlated with irreversible pulpits, with chronical inflammation observed in the histological section of the same tooth.

The visualization of dental pulp morphology and function is very important for treatment decisions [Pretty and Ekstrand, 2016]. From the pulp tissue condition, it could be determined whether non-operative preventive therapies and interventions are sufficient or more surgical treatment measures are necessary like stepwise excavation or indirect pulp capping in case of hyperaemia or reversible pulpitis. It is accepted that the diagnoses irreversible and reversible pulpitis are clinically based terms that are operational, but not biological. Clinical judgement symptoms indicative of irreversible or reversible pulpitis are considered as accurate clinical reflection of the histological picture [Duncan et al., 2019]. In the case of the clinically diagnosed irreversible pulpitis according to radiographical caries depth as well as clinical indicators of caries activity, symptoms, and the results of sensibility tests, it was also observed as the decrease in the MRI T_2 value profile along the pulp, contributing more information for the adequate treatment decision.

Our results interestingly also show that T_2 profiles of teeth in various stages of caries follow the same, flat to slightly decreasing trend in single-rooted teeth and a different, initially increasing and then decreasing, trend in multi-rooted teeth, but with different T_2 offsets depending on the severity of caries. The more dynamic T_2 profiles in multi-rooted teeth than in single-rooted teeth (Fig. 4a, b) can be explained by the non-uniformity of the pulp cross-section area along its length from the coronal to the apical end of the dental pulp. The non-uniformity is more pronounced in multi-rooted teeth due to their high coronal quarter volume and relatively small volume of dental pulp tissue in individual root canals. The high-volume coronal part of the dental pulp in multi-rooted teeth might be more able to compensate caries-induced inflammation processes than the corresponding lower-volume coronal part of the dental pulp in single-rooted teeth. Higher pulp volume enables more reliable measurement of T_2 values with reduced susceptibility effects and absence of the partial volume effect. Therefore, T_2 values in the coronal section of the dental pulp are higher in multi-rooted teeth than in single-rooted teeth. In addition, in multi-rooted teeth, root canals toward the apical part are often not straight and can therefore only partially lie in the imaging slice or

be missing entirely. This can be well seen also in the example in Figure 1b. The problem could be reduced by using multi slice imaging that would enable tracking T_2 values along the entire pulp length. Alternatively, tooth-wide thick slices could be used; however, for the price of resolution loss in the slice direction. In all cases where the dental pulp tissue only partially fills the imaging voxel, we are dealing with the partial volume effect. In general, this occurs whenever there coexist 2 or more different tissue types in one voxel. Due to the partial volume effect, a question remains whether a faster decrease in T_2 values towards the apical part of the dental pulp is actual or a consequence of the partial volume effect. This question can be answered by a T_2 mapping with higher resolution, which in effect reduces the partial volume effect. The examples shown in Figure 2c and d, with lengths of 8.6 and 10.3 mm, are among the longest dental pulps analysed. For other samples, the quality of T_2 maps was practically the same; however, the pulps were simply not that long or other effects, such as an extensive pulp curvature or the partial volume effect, prevented their analysis, especially towards the apical part. In principle, the reading of T_2 becomes unreliable if the MR signal originates from <1 full voxel, which can apply also to other dental pulp parts, not only the apical part. In the coronal part of the pulp, the MR signal reception could in principle be spoiled in cases of metallic (dental amalgam) restorations. From our experience, such restorations do not have any significant effect on the dental pulp MR signal except in the thin interface region (online suppl. Fig. S2). Therefore, metallic restorations were not used as an exclusion criterion for the study, although only one such tooth was included in the present study. More problematic are dental implants because of a larger size and position that extends from the coronal part deep into the jaw bone so that it can spoil MR signal reception from adjacent dental pulps.

Another important advantage of T_2 mapping over ICDAS scoring is the spatially resolved information on the dental pulp response to caries it provides, contrasting with the volume-averaged information supplied by the ICDAS system. In our study, one-dimensional T_2 profiles along the dental pulp were measured, and these enabled analysis of the pulp response to caries along its entire length, that is, from the coronal to the apical part. As can be seen from the results in Table 2, the T_2 profiles provided detection of the pulp decaying processes, being statistically significant mainly in the coronal quarter of the dental pulp and to a lesser extent in the other 3 quarters. In the coronal region, 2nd quarter, and 3rd quarter, the differences were significant between the ICDAS group 6 and all other groups; between the ICDAS group 5 and all other groups, the differences were still significant in the coronal quarter. These results suggest that T_2 mapping is a promising tool for spatially localised detection of the dental pulp response to caries.

MRI is unique among radiological methods as it enables soft tissue imaging with exceptional contrast and with no harmful radiation. However, MRI lacks resolution for applications in dentistry. Moreover, it is relatively slow and, due to the lack of dedicated hardware, still as expensive as other clinical examinations performed on a clinical MRI scanner. This explains why MRI in vivo has thus far been rarely used in dentistry. In MRI, resolution is inevitably associated with sensitivity and scan time. Since the scan time is limited in clinical settings and usually does not exceed 10 min per scan, the only remaining option to increase resolution is to increase sensitivity. This can be done by using a higher-field magnet and a dedicated dental coil. In a 3-T MRI scanner, the increase in signal-to-noise ratio (SNR) is up to 70% compared to a 1.5-T MRI scanner running the same sequence on the same sample [Soher et al., 2007]. The increase is even bigger on research scanners, that is in whole-body 7-T scanners or in systems using small bore vertical magnets where magnetic fields can currently go up to 23 T, but these systems do not allow human in vivo MR imaging. In theory, the increase in SNR with an increasing magnetic field B_0 is proportional to B_0 in larger samples and is proportional to $B_0^{7/4}$ with smaller samples [Hoult and Lauterbur, 1979]. However, in practice such large increase cannot be obtained due to susceptibility effects and reduced T_2 relaxation times at higher fields [Soher et al., 2007]. Sensitivity can be improved also by the use of a coil that would ideally fit into a single tooth or a group of teeth. This way, the filling factor of the detection coil is optimised and consequently an induced voltage in the coil, that is, an NMR signal, is increased. Such dedicated coils for dental applications have already been successfully applied in combination with various MRI sequences: 2D Turbo Spin Echo [Tymofiyeva et al., 2008], SWIFT [Idiyatullin et al., 2014], and FLASH [Flügge et al., 2016; Ludwig et al., 2016]. It has been shown that such coils enable MRI at a reduced field of view and with considerably thinner slices compared to the one in a standard head MRI probe and enable imaging with an isotropic resolution of up to 300 μm. The in-plane resolution of the T_2 mapping in our study was comparable to that, but the slices of 2.5 mm were much thicker. In order to approach the resolution of 300 μm also in the slice direction while not compromising SNR use, a dedicated dental coil is inevitable.

One of the imitations of the present study was that teeth included in the study were not all from different patients and were therefore in principle not independent. On average, approximately 6 teeth from the same patient were included in the study and observed in one examination in the same field of view. This was partly because of the need to maximise the number of studied samples and limited availability of MRI for the study. However, as can be seen from Table 1, teeth of most patients included in the study relatively uniformly covered all ranges of ICDAS scores, so that teeth from each ICDAS group were composed of samples from larger number of patients. In addition, in each ICDAS score group, age distribution of patients was similar. This is important as the pulp tissue volume decreases with age.

In our previous study on characterization of blood clot structure, we compared T_2 mapping with ADC mapping and found ADC mapping more sensitive to tissue changes than T_2 mapping [Vidmar et al., 2010]. In addition, ADC mapping of dental pulp ex vivo [Vidmar et al., 2012] gave very promising results in terms of an excellent correlation between ADC and ICDAS score of the affected dental pulp. Therefore, it is expected that ADC mapping of dental pulp in vivo could be a better choice than T_2 mapping. However, ADC mapping of other body parts than the brain is usually very challenging. The reason for that stems from high sensitivity of the EPI sequence, which is normally used for ADC mapping, to magnetic field homogeneity and body motion. In MRI of teeth, magnetic field homogeneity is poor due to interface regions between hard and soft dental tissues. In addition, patients tend to move the jaws due to accumulating saliva. Our preliminary results on ADC mapping of a dental pulp in vivo using an EPI DWI method were not very promising. In addition to EPI DWI methods, there exist also non-EPI DWI methods, as for example a DWI method based on the single-shot RARE sequence [Alsop, 1997]. This method is considerably less sensitive to magnetic field inhomogeneity and susceptibility effects and could therefore be a much better alternative for DWI/ADC mapping of dental pulp.

Conclusions

This study is, to our knowledge, the first in vivo MRI study aiming to quantify the progression of caries by employing T_2 mapping. The maps were used to obtain T_2 profiles along the dental pulp in teeth at various stages of caries progression. In all cases, it was found that teeth affected by caries have reduced T_2 values. Based on the results of the study, it can be concluded that T_2 values negatively correlate with the severity of caries progression according to the ICDAS score of caries lesion. The method is relatively robust, without the need for the intraoral probe or the radiation exposure and could be executed in clinically relevant time. Therefore, MRI T_2 mapping has a potential to become a complementary diagnostic tool to standard radiographic methods in the assessment of dental pulp response to caries.

Statement of Ethics

The experiments were undertaken with the understanding and written consent of each subject and according to the Declaration of Helsinki (version 2008). The study has been independently reviewed and approved by the Ethical Committee of the National Ministry of Health (Approval number 0120-659/2016/6).

Disclosure Statement

There are no potential conflicts of interest relating to this study.

Funding Sources

This work was supported by Grant No.: P3-0019, Ministry of Higher Education, Science and Technology, Slovenia.

References

Alsop DC. Phase insensitive preparation of single-shot RARE: application to diffusion imaging in humans. Magn Reson Med. 1997 Oct;38(4):527–33.

Assaf AT, Zrnc TA, Remus CC, Khokale A, Habermann CR, Schulze D, et al. Early detection of pulp necrosis and dental vitality after traumatic dental injuries in children and adolescents by 3-Tesla magnetic resonance imaging. J Craniomaxillofac Surg. 2015 Sep;43(7):1088–93.

Bohnen S, Radunski UK, Lund GK, Ojeda F, Looft Y, Senel M, et al. Tissue characterization by T1 and T2 mapping cardiovascular magnetic resonance imaging to monitor myocardial inflammation in healing myocarditis. Eur Heart J Cardiovasc Imaging. 2017 Jul;18(7):744–51.

Cankar K, Nemeth L, Bajd F, Vidmar J, Serša I. Discrimination between intact and decayed pulp regions in carious teeth by ADC mapping. Caries Res. 2014;48(5):467–74.

Drăgan OC, Fărcăşanu AS, Câmpian RS, Turcu RV. Human tooth and root canal morphology reconstruction using magnetic resonance imaging. Clujul Med. 2016;89(1):137–42.

Duncan HF, Galler KM, Tomson PL, Simon S, El-Karim I, Kundzina R, et al.; European Society of Endodontology (ESE) developed by. European Society of Endodontology position statement: management of deep caries and the exposed pulp. Int Endod J. 2019 Jul;52(7):923–34.
Farges JC, Alliot-Licht B, Renard E, Ducret M, Gaudin A, Smith AJ, et al. Dental pulp defence and repair mechanisms in dental caries. Mediators Inflamm. 2015;2015:230251.
Flügge T, Hövener JB, Ludwig U, Eisenbeiss AK, Spittau B, Hennig J, et al. Magnetic resonance imaging of intraoral hard and soft tissues using an intraoral coil and FLASH sequences. Eur Radiol. 2016 Dec;26(12):4616–23.
Gaudino C, Cosgarea R, Heiland S, Csernus R, Beomonte Zobel B, Pham M, et al. MR-Imaging of teeth and periodontal apparatus: an experimental study comparing high-resolution MRI with MDCT and CBCT. Eur Radiol. 2011 Dec;21(12):2575–83.
Hoult DI, Lauterbur PC. Sensitivity of the zeugmatographic experiment involving human samples. J Magn Reson. 1979;34:425–33.
Hövener JB, Zwick S, Leupold J, Eisenbeiβ AK, Scheifele C, Schellenberger F, et al. Dental MRI: imaging of soft and solid components without ionizing radiation. J Magn Reson Imaging. 2012 Oct;36(4):841–6.
Idiyatullin D, Corum C, Moeller S, Prasad HS, Garwood M, Nixdorf DR. Dental magnetic resonance imaging: making the invisible visible. J Endod. 2011 Jun;37(6):745–52.
Idiyatullin D, Corum CA, Nixdorf DR, Garwood M. Intraoral approach for imaging teeth using the transverse B1 field components of an occlusally oriented loop coil. Magn Reson Med. 2014 Jul;72(1):160–5.
Ludwig U, Eisenbeiss AK, Scheifele C, Nelson K, Bock M, Hennig J, et al. Dental MRI using wireless intraoral coils. Sci Rep. 2016 Mar;6(1):23301.
Martin FE. Carious pulpitis: microbiological and histopathological considerations. Aust Endod J. 2003 Dec;29(3):134–7.
Mjör IA. Pulp-dentin biology in restorative dentistry. Part 7: the exposed pulp. Quintessence Int. 2002 Feb;33(2):113–35.
Murray PE, Lumley PJ, Smith AJ. Preserving the vital pulp in operative dentistry: 3. Thickness of remaining cavity dentine as a key mediator of pulpal injury and repair responses. Dent Update. 2002 May;29(4):172–8.
Pitts N. "ICDAS"—an international system for caries detection and assessment being developed to facilitate caries epidemiology, research and appropriate clinical management. Community Dent Health. 2004 Sep;21(3):193–8.
Pitts NB. Modern perspectives on caries activity and control. J Am Dent Assoc. 2011 Jul;142(7):790–2.
Pretty IA, Ekstrand KR. Detection and monitoring of early caries lesions: a review. Eur Arch Paediatr Dent. 2016 Feb;17(1):13–25.
Soher BJ, Dale BM, Merkle EM. A review of mr physics: 3t versus 1.5t [v.]. Magn Reson Imaging Clin N Am. 2007 Aug;15(3):277–90.
Sustercic D, Sersa I. Human tooth pulp anatomy visualization by 3D magnetic resonance microscopy. Radiol Oncol. 2012 Mar;46(1):1–7.
Tymofiyeva O, Boldt J, Rottner K, Schmid F, Richter EJ, Jakob PM. High-resolution 3D magnetic resonance imaging and quantification of carious lesions and dental pulp in vivo. MAGMA. 2009 Dec;22(6):365–74.
Tymofiyeva O, Rottner K, Gareis D, Boldt J, Schmid F, Lopez MA, et al. In vivo MRI-based dental impression using an intraoral RF receiver coil. Concept Magn Reson. 2008;33B(4):244–51.
Vidmar J, Blinc A, Sersa I. A comparison of the ADC and T2 mapping in an assessment of blood-clot lysability. NMR Biomed. 2010 Jan;23(1):34–40.
Vidmar J, Cankar K, Nemeth L, Serša I. Assessment of the dentin-pulp complex response to caries by ADC mapping. NMR Biomed. 2012 Sep;25(9):1056–62.
Vlaardingerbroek MT. Boer JAd: Magnetic resonance imaging : Theory and practice. Berlin, New York: Springer; 1996. https://doi.org/10.1007/978-3-662-03258-9.
Weiger M, Pruessmann KP, Bracher AK, Köhler S, Lehmann V, Wolfram U, et al. High-resolution ZTE imaging of human teeth. NMR Biomed. 2012 Oct;25(10):1144–51.
Zero DT, Zandona AF, Vail MM, Spolnik KJ. Dental caries and pulpal disease. Dent Clin North Am. 2011 Jan;55(1):29–46.